CHAPTER ONE

The Formation of Amorphous Solids

1.1 FREEZING INTO THE SOLID STATE: GLASS FORMATION VERSUS CRYSTALLIZATION

To begin with, let us suppose that we all know what is meant by the term "solid." (This innocent assumption is less harmless than it appears, and it calls for a bit of discussion, which is to be supplied in Section 1.3.) In a familiar type of thought experiment, often invoked to conceptually analyze the energetics involved in the formation of a solid, a large collection of initially isolated atoms is gradually brought together "from infinity" until the actual interatomic spacings of the solid are attained. The actual experiment that most closely corresponds to this gedanken experiment involves cooling the vapor of the material until it condenses into the liquid state, and then further gradual cooling of the liquid until it solidifies. Results of such an experiment, for a given quantity of the material, may be represented on a volume-versus-temperature $V(T)$ plot such as the one schematically shown in Fig. 1.1.

Figure 1.1 should be read from right to left, since time runs in that direction during the course of the quenching (temperature-lowering) experiment. A sharp break or bend in $V(T)$ marks a change of phase occurring with decreasing temperature. The first occurs when the gas (whose volume is limited only by the dimensions of the experimental enclosure) condenses to the liquid phase (of well-defined volume, but shape enclosure-determined) at the boiling temperature T_b. Continued cooling now decreases the liquid volume in a continuous fashion, the slope of the smooth $V(T)$ curve defining the liquid's volume coefficient of thermal expansion $\alpha = (1/V)\,(\partial V/\partial T)_P$. (The experiment is assumed to be taking place at low pressure, $P \approx 0$.) Eventually, when the temperature is brought low enough, a liquid→solid transition takes place (with the exception of liquid helium, which remains liquid as $T \to 0$ in the absence of pressure). The solid then persists to $T = 0$, its signature in terms of $V(T)$ being a small slope corresponding to the low value (relative to that of the liquid phase) of the expansion coefficient α which characterizes a solid.

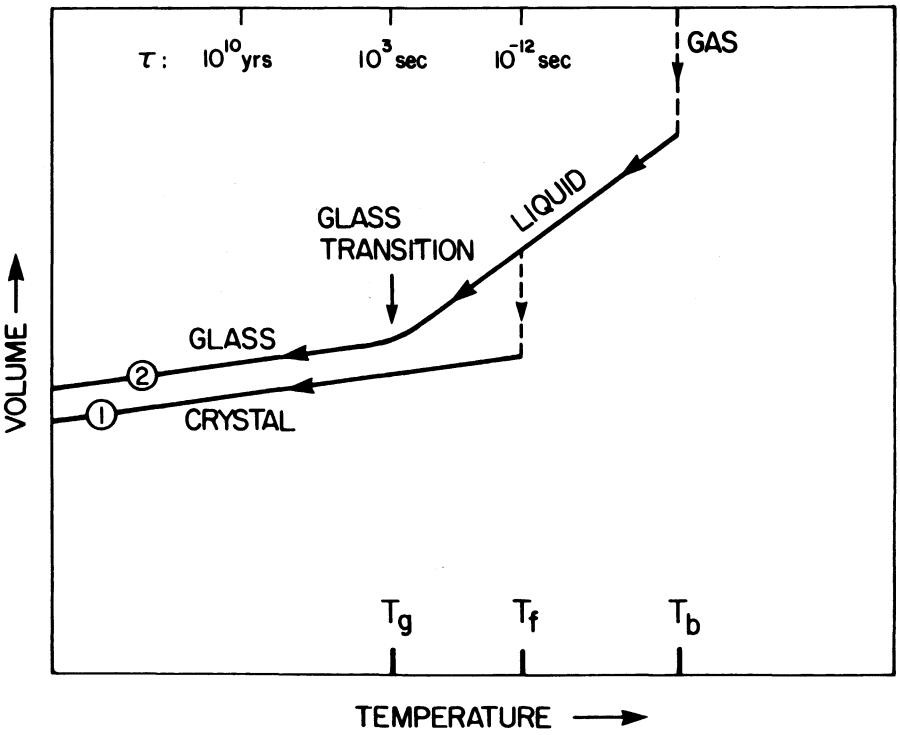

Figure 1.1 The two general cooling paths by which an assembly of atoms can condense into the solid state. Route ① is the path to the crystalline state; route ② is the rapid-quench path to the amorphous solid state.

A liquid may solidify in two ways:

1. *discontinuously* to a crystalline solid or
2. *continuously* to an amorphous solid (glass).

The two solids resulting from these two quite different solidification scenarios are labeled, correspondingly, ① and ② in Fig. 1.1. Scenario ① occurs in Fig. 1.1 at temperature T_f, the freezing (or melting) point. The liquid→crystal transition is marked by a discontinuity in $V(T)$, an abrupt contraction to the volume of the crystalline solid. In a quenching experiment carried out at a sufficiently low cooling rate, this is usually the route taken to arrive at the solid state. But at sufficiently high cooling rates, it is found that most materials alter their behavior and follow route ② to the solid phase. T_f is bypassed without incident, and the liquid phase persists until a lower temperature T_g is reached. Here the second solidification scenario is realized. The liquid→glass transition occurs in a narrow temperature interval near T_g, the *glass transition* temperature. There is no volume discontinuity, instead V(T) bends over to acquire the small slope (similar to that of the crystal) characteristic of the low thermal expansion of a solid.

Both crystals and glasses are bona fide solids and share the essential attributes of the solid state (Section 1.3). Their fundamental difference is in the basic nature of their microscopic, atomic-scale structure. In crystals, the equilibrium positions of the atoms form a translationally periodic array. The atomic positions exhibit long-range order. In amorphous solids, long-range order is absent; the array of equilibrium atomic positions is strongly disordered. For crystals, the atomic-scale structure is securely known at the outset from the results of diffraction experiments, and it provides the basis for the analysis of such properties as electronic and vibrational excitations. For amorphous solids, the atomic-scale structure is itself one of the key mysteries. Several chapters of this book are devoted to the structure of glasses. A brief preview is given in Section 1.3 and Fig. 1.6.

A note on terminology is in order at this point. The term *amorphous solid* is the general one, applicable to any solid having a nonperiodic atomic array as outlined above. The term *glass* has conventionally been reserved for an amorphous solid actually prepared by quenching the melt, as in ② of Fig. 1.1. Since, as discussed in Section 1.2, there are other ways to prepare amorphous solids than by melt-quenching, glass (in the conventional usage) is the more restrictive term. In this book, that historical distinction will not be adhered to, and both terms will be used synonymously. (''Historical'' is used here in two senses, since the distinction itself refers to the history, i.e., method of preparation, of the solid.) Not only does this lubricate the discussion because ''glass'' is one word while ''amorphous solid'' is two, it is also convenient to have ''glass'' to set in opposition to ''crystal'' (instead of ''amorphous solid'' versus ''crystalline solid''). Other terms, sometimes used in the literature in place of amorphous solid, are noncrystalline solid and vitreous solid.

A detailed view of the vicinity of the liquid→glass solidification transition is shown in Fig. 1.2 for the case of the organic glass polyvinylacetate ($CH_2CHOOCCH_3$). The data show results for $V(T)$ obtained at two different cooling rates, and reveal that the observed transition temperature T_g depends upon the cooling rate at which the experiment is carried out. This is a characteristic *kinetic* dimension of the glass transition. The two $V(T)$ curves in Fig. 1.2 are labeled by two experimental time scales, 0.02 hr for the upper curve and 100 hr for the lower curve. In these particular experiments, the stated times are the times elapsed in quenching the specimen to temperature T from a fixed initial temperature well above T_g. Note that the effect of changing this time by a factor of 5000 is to shift T_g by only 8°K. Thus this effect, while quite real, is small.

Denoting the average cooling rate $-\overline{dT/dt}$ by $\dot{T}$, the mild influence that the time scale of the measurement exerts on the experimentally observed liquid→glass temperature may be indicated by writing T_g as $T_g(\dot{T})$. The weak functional dependence may be approximated as a logarithmic one. Typically, changing $\dot{T}$ by an order of magnitude causes T_g to shift by a few degrees kelvin.

The reason that T_g shifts to lower temperatures when the cooling process is extended over longer times resides in the temperature dependence of a typical

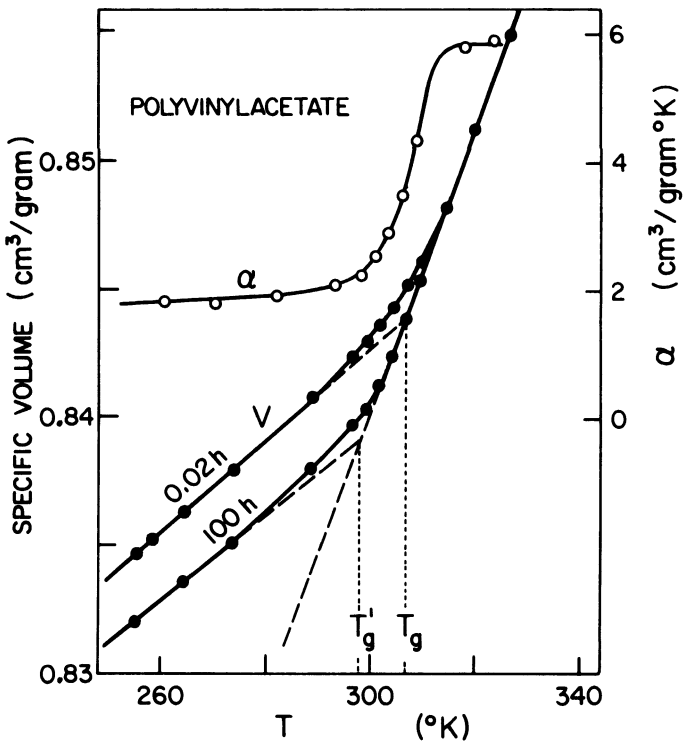

Figure 1.2 Volume-versus-temperature cooling curves for an organic material in the neighborhood of the glass transition. $V(T)$ is shown for two greatly different cooling rates, as is the coefficient of thermal expansion $\alpha(T)$ for the fast-cooling curve (0.02 hr). The break in $V(T)$, and the corresponding step in $\alpha(T)$, signal the occurrence of the liquid→glass transition (after Kovacs, Hutchinson, and Aklonis, 1977).

molecular relaxation time τ. (The adjective "typical" reflects the fact that there is actually a spectrum of relaxation times; τ may be regarded as the geometric mean of that distribution.) The quantity $1/\tau$ characterizes the rate at which the molecular configuration (atomic-scale structure) of the condensed system adapts itself to a change in temperature. This quantity varies enormously during the cooling process. An indication of this dramatic variation is given at the top of Fig. 1.1 where, in crude order-of-magnitude terms, values of τ are associated with three temperatures: T_f, T_g, and a temperature well below T_g (say, T_g – 50°K). The structural-rearrangement response time may increase from the order of 10^{-12} sec at T_f to 10^{10} years (age of the universe) at T_g – 50°K. (Experimentally, τ is accessible at high temperatures where it roughly scales inversely as the viscosity of the liquid. At low temperatures, in the solid, τ is inferred indirectly.)

The 30 orders of magnitude in τ, spanned between the liquid near the melting point and the glass well below the "glass point," are swept through

swiftly and continuously at temperatures in between. As T traverses the region near T_g, $\tau(T)$ becomes comparable to the time scale of the measurement (typically 10^3 sec, give or take an order of magnitude or two). As T is lowered below T_g, τ becomes much larger than any experimentally accessible times, so that the material loses its ability to rearrange its atomic configuration in harmony with the imposed decline of temperature. The atoms get frozen into well-defined positions (equilibrium positions, about which they oscillate), which correspond to the configuration they had at T_g. It is now easy to understand why, in Fig. 1.2, expanding the experimental time scale (slowing the cooling rate $\dot{T}$) lowers the observed glass point T_g: If a longer experimental time t is available, then a lower temperature T is needed to achieve the condition $\tau(T) > t$ which freezes the atoms into the configuration that they maintain in the amorphous solid state. Note that the mildness of the t dependence of T_g is simply the other side of the coin with respect to the severity of the exceedingly steep function $\tau(T)$.

While kinetic effects clearly play a role in the operational definition of T_g, it is generally believed that the observed liquid↔glass transition is a manifestation of an underlying thermodynamic transition viewed as corresponding to the limit $t \to \infty$, $\dot{T} \to 0$. Some of the experimental evidence of this is given in Section 1.4, and theories of the glass transition—which has been one of the knottiest problems in condensed matter physics—will be discussed in Chapter Four.

In addition to showing what happens to the specific volume (inverse of the density) at temperatures near T_g, Fig. 1.2 also includes a related thermodynamic variable, the expansion coefficient α. This quantity experiences a well-defined "step" near T_g, corresponding to the slope change in $V(T)$. Other thermodynamic aspects of T_g are discussed in Section 1.4.

A comment should be made about the terms "freezing" and "melting." These two terms are conventionally reserved for the two directions (← and →) in which a material may traverse the crystal↔liquid transition, the event which occurs at T_f along route ① of Fig. 1.1. This usage is usually adhered to here. But it should be realized that the same terms *also* describe the event that occurs at T_g along route ② of Fig. 1.1. For the glass↔liquid transition, T_g denotes the temperature at which (in direction ←) the undercooled liquid freezes. In the other direction (→, increasing temperature), T_g denotes the temperature *at which the glass melts*.

1.2 PREPARATION OF AMORPHOUS SOLIDS

For a long time it was thought that only a relatively restricted number of materials could be prepared in the form of amorphous solids, and it was common to refer to these "special" substances (e.g., oxide glasses and organic polymers) as "glass-forming solids." This notion is wrong, and it is now realized that "glass-forming ability" is almost a universal property of condensable matter. The amorphous solid state is ubiquitous. Table 1.1 presents a list of

TABLE 1.1 Representative amorphous solids, their bonding types, and their glass-transition temperatures

Glass	*Bonding*	T_g (°K)
SiO_2	Covalent	1430
GeO_2	Covalent	820
Si, Ge	Covalent	—
$Pd_{0.4}Ni_{0.4}P_{0.2}$	Metallic	580
BeF_2	Ionic	570
As_2S_3	Covalent	470
Polystyrene	Polymeric	370
Se	Polymeric	310
$Au_{0.8}Si_{0.2}$	Metallic	290
H_2O	Hydrogen bonded	140
C_2H_5OH	Hydrogen bonded	90
Isopentane	van der Waals	65
Fe, Co, Bi	Metallic	—

amorphous solids in which every class of bonding type is represented. The glass-transition temperatures span a wide range.

The correct viewpoint (expressed, for example, in D. Turnbull's 1969 review paper) is the following: *Nearly all materials can, if cooled fast enough and far enough, be prepared as amorphous solids.* ("Fast" and "far" are explained below.) This viewpoint has been abundantly supported in recent years by the preparation of an enormous variety of amorphous solids. Prominent among these, and providing one of the most striking demonstrations of the ubiquity of this state of condensed matter, are the metallic glasses. Because metals tend to be structurally simple materials (many form, in the crystalline state, close-packed structures), the proliferation of glassy metals is a very significant development. Traditional "glass formers" have been materials associated with considerable complexity on a molecular scale, such as organic glasses composed of polymer chains having bulky sidegroups dangling from them. Metals had been thought to be too simple to form glasses.

Figure 1.3 displays an effective technique, known as *melt spinning*, for achieving the very high rate of cooling needed to form a metallic glass. A jet of hot molten metal is propelled against the surface of a rapidly rotating copper cylinder, which is kept cool (room temperature or below). The liquid metal is drawn into a thin film, roughly 50 microns thick (50 μm = 0.05 mm). Since the film is so thin, since it is in intimate contact with a large heat sink, and since metals have high thermal conductivity, the liquid cools and solidifies extremely fast. A temperature drop of about 1000°K is accomplished in about a millisecond, i.e., $\dot{T} \approx 10^6$ °K/sec. The solid film of metallic glass is spun off the rotor, as a continuous ribbon, *at a speed exceeding 1 kilometer per minute.*

Thus the name of the game—the essential ingredient in the preparation of an amorphous solid—is *speed.* A given material may solidify via either of the

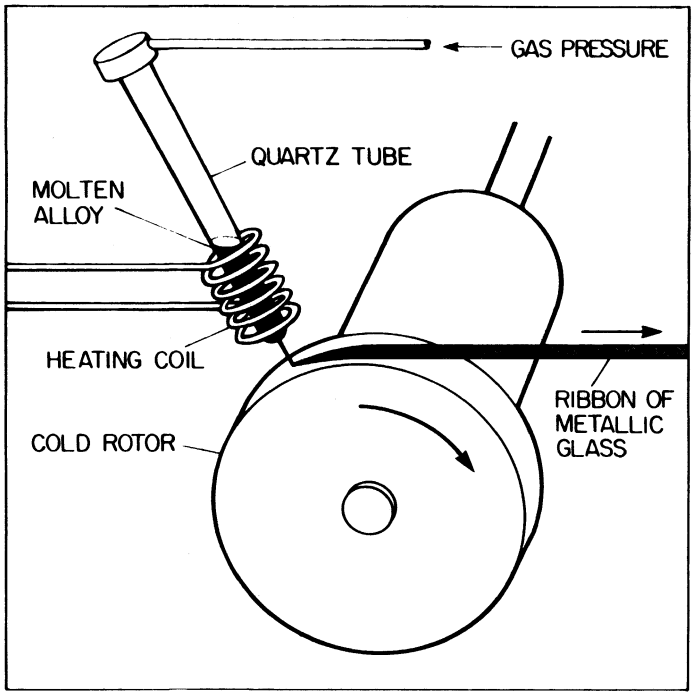

Figure 1.3 Melt spinning of metallic glass. The solid ribbon of amorphous metal is spun off at speeds that can exceed 1 kilometer per minute (from Chaudhari, Giessen, and Turnbull, 1980, copyright 1980 by Scientific American, Inc., all rights reserved, used by permission).

two routes indicated in Fig. 1.1. As soon as the temperature of the liquid is lowered to T_f, it may take route ① to the solid state and crystallize. But crystallization takes time. Crystalline centers must form (a process called nucleation) and then grow by outward propagation of the crystal/liquid interfaces. With the liquid being cooled at a finite rate, the liquid may be taken below T_f along the $V(T)$ trajectory which smoothly continues the curve from higher temperatures. In the temperature interval between T_f and T_g, the liquid is referred to as the undercooled or supercooled liquid. (The undercooled liquid is still unambiguously *liquid* and must not be confused with the glass, as is mistakenly done in a few texts.) If its temperature can be taken below T_g before crystallization has had time to occur, the undercooled liquid solidifies as the glass and remains in this form essentially indefinitely.

Glass formation, therefore, is a matter of *bypassing crystallization*. The channel to the crystalline state is evaded by quickly crossing the dangerous regime of temperature between T_f and T_g and achieving the safety of the amorphous solid state below T_g. Throughout the temperature interval $T_g < T < T_f$, the liquid is "at risk" with respect to nucleation and growth of crystallites. Earlier it was stated that, for a material to be prepared as an amorphous solid, cooling must

proceed "fast enough and far enough." "Far enough" is seen to mean that the quench must be taken to $T < T_g$, and "fast enough" means that $T_g < T < T_f$ must be crossed in a time too short for crystallization to occur. In contrast to crystallization, which is heterogeneous (pockets of the solid phase appear abruptly within the liquid and then grow at its expense), the liquid→glass transformation occurs homogeneously throughout the material. This transformation would be observed for any liquid when sufficiently undercooled (i.e., all liquids would form glasses), except for the intervention of crystallization.

"Fast enough" can be, for many materials, very much slower than the quenching rate ($\dot{T} \approx 10^6$ °K/sec) quoted in connection with Fig. 1.3. Unlike the single millisecond taken to quench a metallic glass, the time taken to quench the silicate glass that forms the rigid ribbed disk of the Mt. Palomar telescope was eight months, corresponding to a leisurely $\dot{T}$ of 3×10^{-5} °K/sec. It is much easier to prepare a glass for which a low $\dot{T}$ suffices than it is to prepare one for which a high $\dot{T}$ is needed. Thus, while it is not meaningful to speak of glass-forming solids (since this classification encompasses virtually all materials), it is certainly valid to refer to *glass-forming tendency*. This attribute is correlated with $1/\dot{T}$, and is obviously much greater for oxide glasses than for metallic glasses.

Figure 1.4 schematically illustrates four techniques for preparing amorphous solids that span the range of quenching rates. These techniques are not fundamentally different from those used for preparing crystalline solids; the point is simply that care is taken to quench fast enough to form the glass rather than slow enough to form the crystal.

For materials with very high glass-forming tendency, the melt can be allowed to cool slowly by simply turning off the furnace or by bringing it down in a programmed manner (Fig. 1.4*a*). Typical cooling rates are in the range from 10^{-4} to 10^{-1} °K/sec. Glasses in this category, among those listed in Table 1.1, are SiO_2, As_2S_3, and polystyrene. Thus, although the crystalline form of As_2S_3 is abundant in nature (which had a long time to produce it) as the mineral orpiment, synthetic crystals cannot be prepared from the melt on any experimentally reasonable time scale. The melt always solidifies as the amorphous solid.

Somewhat faster rates are needed to quench a glass such as amorphous selenium, an elemental glass composed of long-chain polymeric molecules. Using an ice-water bath to quench modest volumes of the melt, as indicated in Fig. 1.4*b*, yields rates in the range 10^1–10^2 °K/sec. Se glass can be prepared by this method, as can the Pd-Ni-P metallic glass included in Table 1.1. This metallic glass has a glass-forming tendency high enough to allow it to be prepared in bulk form, rather than the thin-film form characteristic of the other metallic glasses listed in the table.

The technique sketched in Fig. 1.4*c* is another of the melt-quenching methods (of which the melt-spinning method of Fig. 1.3 is the most spectacular example) developed specifically for metallic glasses. These methods are collectively called *splat-quenching* techniques, and achieve $\dot{T}$ values in the range 10^5–10^8 °K/sec. The hammer-and-anvil drop-smasher method of Fig. 1.4*c*

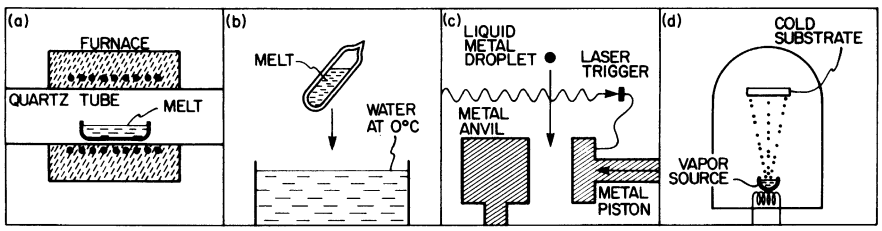

Figure 1.4 Four methods of forming amorphous solids: (*a*) slow cooling, (*b*) moderate quenching, (*c*) rapid "splat-quenching", and (*d*) condensation from the gas phase.

cools the liquid droplet from two sides at once, and is used to produce milligram-size laboratory specimens of metallic glasses such as the Au-Si alloy listed in Table 1.1.

Before going on to discuss condensation from the vapor phase (Fig. 1.4*d*), it is interesting to take note of a final method for quenching the liquid, one which is even faster than splat quenching. The technique is called *laser glazing*, and it begins with the material in crystalline form. A very short and very intense single laser pulse is focused onto a very small spot on the crystal surface, with the laser wavelength selected so that the light energy is absorbed in an extremely thin (~ 100 Å) layer of the solid. The large energy dumped into this tiny volume is sufficient to melt it, but it is swiftly quenched and resolidified by the surrounding crystal. The small, very thin, melted-and-quenched region has been found to be amorphous in the case of silicon, a material normally preparable in amorphous form only by vapor-condensation techniques. Amorphous metals can also be prepared by laser glazing. The quench rate can only be roughly estimated by highly approximate calculations; these yield towering $\dot{T}$ values in the range 10^{10}–10^{12} °K/sec.

All of the glass-forming methods discussed thus far rely upon speed-induced access to route ② of Fig. 1.1. In Fig. 1.4*d*, we show a representative of a class of techniques that bypasses the liquid phase completely and constructs the amorphous solid in atom-by-atom fashion from the gas phase. These techniques possess the highest effective quench rates ($\dot{T}$ is probably too high to be any longer a meaningful parameter in its original sense), and they are widely used to prepare glasses which have not been obtained by melt-quenching methods.

Figure 1.4*d* shows the simplest of these *vapor-condensation* techniques. A vapor stream, formed within a vacuum chamber by thermal evaporation of a sample ("source") of the material in question, impinges upon the surface of cold substrate. As the atoms condense on the surface, the as-deposited amorphous structure is quenched in if conditions are arranged so that their thermal energy is extracted from them before they can migrate to the crystalline configuration. Variations of the method involve vaporizing the source by the use of an electron beam, or the use of ion bombardment to drive atoms from it. Another method involves the plasma-induced decomposition of a molecular

species, a technique employed to deposit amorphous silicon from silane (SiH_4) vapor.

Vapor-condensation techniques produce amorphous solids in the form of thin films, typically 5–50 μm thick. Among the amorphous solids listed in Table 1.1, those which normally demand vapor-condensation methods for their preparation are Si, Ge, H_2O, and the elemental metallic glasses Fe, Co, and Bi. For the pure metals, the substrate must be kept very cold ($<20°K$). It is usually difficult to define T_g for such glasses, since they are not prepared by a liquid→glass quenching process and, when subjected to a heating cycle after preparation, they often crystallize before there is a chance for the glass→liquid transition to occur.

Many glasses which may be formed by melt quenching, such as Se and As_2S_3, are often prepared instead by vapor deposition when thin films are desired (as in applications such as xerography, Section 1.5). Some differences between melt-quenched and vapor-quenched material can be detected, but these normally disappear when the latter is allowed to anneal (Section 3.1.2). It is correct to regard both techniques as producing essentially the same condensed phase.

A trend exists for glass-forming tendency to be greater for a binary material (say, a silicon–gold alloy) than for an elemental one (say, pure silicon). This has to do with the relation between T_g and T_f. Figure 1.5 shows the relevant aspect of the temperature-versus-composition phase diagram for the binary system $Au_{1-x}Si_x$. For the alloy ($0 < x < 1$), the liquid is stabilized and thus the melting point T_f is lowered, relative to that of the single-component endpoints ($x = 0$ or 1), by the entropy of mixing and the attractive interaction between the two components. There is seen to be a eutectic composition $x = 0.2$ at which the melting point is minimized at a deep cusp in $T_f(x)$. At $x = 0.2$, T_g/T_f takes on its largest value, which is about 0.5 for this system. (For comparison, in excellent glass formers such as As_2S_3 and SiO_2, T_g/T_f is about 0.7.)

Near the eutectic composition, as at *a* in the figure, a liquid is much more readily quenched to the glass than is a liquid at a distant composition such as *b*. The treacherous territory between T_f and T_g, within which the melt is both thermodynamically ($T < T_f$) *and* kinetically ($T > T_g$) capable of crystallizing, is much broader and more forbidding at *b* than at *a*. Thus the eutectic composition is favored for glass formation, a conclusion consistent with the observation that $Au_{0.8}Si_{0.2}$ can be splat quenched to the glassy state while Au and Si cannot. Pure silicon can be vapor quenched to form the amorphous form, while pure gold has yet to be prepared as an amorphous solid. The latter eventuality is, to end on a note in keeping with the theme of this section, *simply a matter of time.*

1.3 STRUCTURE, SOLIDITY, AND RESPECTABILITY

The title of this section mentions three attributes of amorphous solids, each of which will be discussed in turn. The first two are physical attributes; the third is

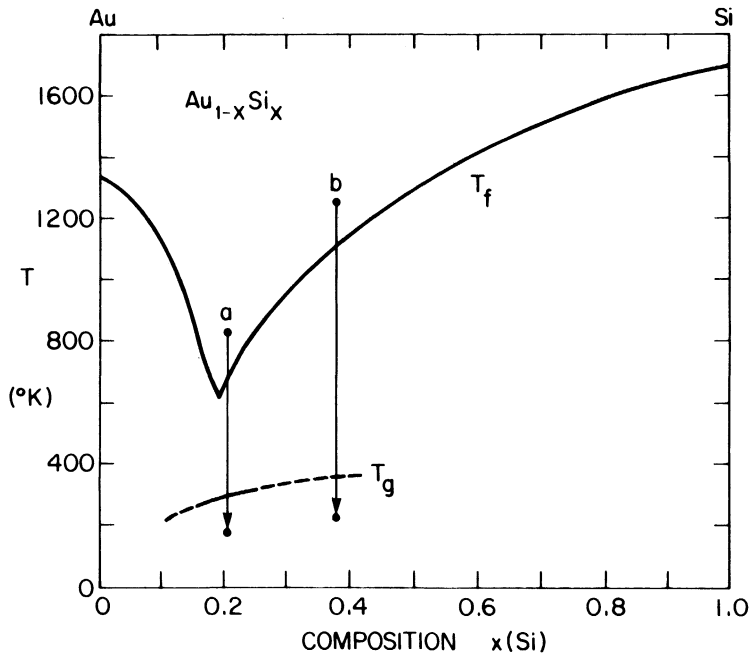

Figure 1.5 Glass formation in the gold–silicon system. Two quenches from the liquid state, at two compositions, are indicated. Glasses can be prepared much more readily in quench *a* than in quench *b*, since the latter must cross a greater temperature range between T_f and T_g in which it is "at risk" vis-à-vis crystallization. (The T_f curve is from the work of Predel and Bankstahl, 1975; the T_g curve is from the work of Chen and Turnbull, 1968.)

a different type of quality, only recently attributed to glasses in conventional attitudes about what constitutes the discipline of solid-state physics.

The subject of structure dominates the following two chapters, but it seems advisable to insert a brief preview at this point. Figure 1.6 presents, schematically and in a nutshell, the salient characteristics of the atomic arrangements in glasses as opposed to crystals. Also included, as an additional and useful reference point, is a sketch of the arrangement in a gas. Of necessity, two-dimensional crystals, glasses, and gases are represented, but the essential points to be noted carry over to their actual, three-dimensional, physical counterparts. For the two sketches representing ideal crystal (*a*) and glass (*b*) lattices, the solid dots denote the equilibrium positions about which the atoms oscillate; for the gas (*c*), the dots denote a snapshot of one configuration of instantaneous atomic positions.

For an amorphous solid, the essential aspect with which its structure differs with respect to that of a crystalline solid is *the absence of long-range order.* There is no translational periodicity. This fundamental difference is evident at a glance in Figs. 1.6*a* and 1.6*b*.

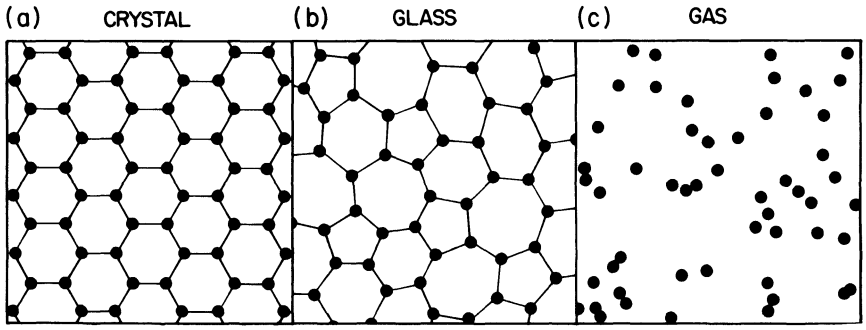

Figure 1.6 Schematic sketches of the atomic arrangements in (*a*) a crystalline solid, (*b*) an amorphous solid, and (*c*) a gas.

On the other hand, the atomic positions in the glass are *not* randomly distributed in space. Randomness is a trait more properly associated with Fig. 1.6*c*, at least in the low-density limit in which the atoms comprising the gas may be viewed as point particles. For such a dilute gas (the ideal gas of the kinetic theory), the particle positions are totally uncorrelated. Each atom may be located anywhere, independent of the positions of all other atoms. But in Fig. 1.6*b*, there is seen to be a high degree of *local* correlation. Each atom has (in the example used here for illustration) three nearest neighbors at nearly the same distance from it. Nearest-neighbor atoms are connected by lines in the figure, and the "bond angles"—formed where these lines meet at an atomic position—are also nearly equal.

In the crystalline case of Fig. 1.6*a*, the nearest-neighbor separations and bond lengths are *exactly* equal (remember that we are dealing with the equilibrium positions), rather than *nearly* equal as in the glass. The degree of local correlation in amorphous solids is quantitatively described in the following chapters; it suffices here to say that this local order is quite high. Thus glasses have, in common with crystals, *a high degree of short-range order.* As in crystals, this is a consequence of the chemical bonding responsible for holding the solid together.

Thus, while the lack of long-range order in glasses implies randomness at large separations (knowing the positions of a few atoms does *not* help to locate, as it *does* in a crystal, the positions of distant atoms), the atomic-scale structure is highly nonrandom for a few interatomic distances about any given atom. A simple thought experiment serves as one way of demonstrating (other than by just looking) the presence of local order in Figs. 1.6*a* and 1.6*b* and its absence in Fig. 1.6*c*. Suppose a single atom is plucked out of each panel of the figure by a man with a bad memory. If he later wished to reinsert each atom in its original position, he would have no difficulty doing so for Figs. 1.6*a* and 1.6*b*. Not so, however, for Fig. 1.6*c*; since it is completely random, the remaining atomic positions provide no clue about the missing one.

Since Fig. 1.6*c* is a genuinely random array while Fig. 1.6*b* is not, it may seem surprising that all three main categories of amorphous-solid structure discussed in the next chapters (random close packing, continuous random network, random-coil model) include the term random in their names. This can be accepted as a historical circumstance, but we may also agree that random applies in the limited sense of referring to *statistical distributions*, which describe quantities (such as bond angles) in the glass structure that would take on a *single* fixed value in the crystal.

The difference between Figs. 1.6*c* and 1.6*b* can be characterized as a case of *unconstrained* versus *constrained chance.* A random array of point particles, unconstrained by any particle–particle correlations, is a suitable model for a gas at low density, but the disorder in a glass is constrained at short distances by the physics and chemistry of the atom–atom bonding interactions. This dichotomy evokes a philosophical analogy which I cannot resist mentioning. Physics and mathematics can be viewed, respectively, as constrained and unconstrained logical systems. In mathematics the system is largely unconstrained by considerations other than logical consistency, but physical theory is additionally, and essentially, disciplined by the *experimental* requirement that it be (in Einstein's words) "of value for the comprehension of reality."

Before leaving Fig. 1.6*b*, we should note the term *topological disorder* (treated further in Chapter Two) in connection with the glass structure schematically represented here. *This disorder is intrinsic to the lattice structure itself.* It is a much more severe class of disorder than that mentioned in the next paragraph.

There are certain types of crystalline systems that are sometimes classified as disordered solids because, while their crystal lattices remain intact and fundamentally resemble Fig. 1.6*a*, their translational symmetry is broken by the chemical (for a "mixed crystal") or orientational (for a "plastic crystal") identity of the objects which occupy the lattice sites. In a mixed crystal such as Ge_xSi_{1-x}, we know *where* each atom is (on a site of the crystalline diamond lattice, shown later in Fig. 2.10), but we do not know *what* it is (Ge or Si). Each lattice site is occupied at random by either a Ge atom (with probability x) or a Si atom (with probability $1 - x$). In a "plastic crystal," symmetric molecules set in different orientations sit on the sites of a periodic lattice. The disorder in such systems (*compositional disorder* for a mixed crystal, *rotational disorder* for a plastic crystal) is very mild compared to the topological disorder characteristic of amorphous solids, because there remains an underlying crystal lattice with its periodicity preserved, and it is often possible to deal with such solids by conventional methods of crystal physics. Thus, the electronic and optical properties of Ge_xSi_{1-x} mixed crystals may be adequately approximated by the "virtual crystal approximation," in which the solid is viewed as a perfectly periodic crystal composed of a single type of fictitious atom that is intermediate in behavior to germanium and silicon. Such mildly-disordered essentially-crystalline solids are not treated in this book.

To move on to the second topic of this section, the subject of solidity, we now consider what *time* does to the configurations represented in Fig. 1.6. For

Fig. 1.6*c*, the effect of letting the clock run is to completely overturn the particular instantaneous structure shown here for the gas. The motion of the atoms takes the gas into other random arrays that, on the scale of atomic dimensions, are totally different from the specific arrangement of Fig. 1.6*c*. (On a macroscopic scale, of course, the effect is that of a small statistical fluctuation on, say, the density.) That atomic motion, for a dilute gas, consists of straight-line trajectories which are punctuated occasionally by sharp deflections corresponding to collisions of the atoms with each other or with the walls of the container.

Time has no such drastic effect on the structures represented in Figs. 1.6*a* and 1.6*b*. While plenty of motion is going on (even at 0°K, the zero-point motion remains), this motion does *not* overthrow the structure in a crystal or a glass. Viewing a given atom as a classical particle with a definite trajectory, the situation is as sketched in Fig. 1.7*a*. The atom stays close to a well-defined equilibrium position, and executes oscillatory motion about it. This persistent aspect is in marked contrast to the fluid scene in Fig. 1.6*c*, in which the motion is translational on an atomic scale.

An essential distinction is thereby drawn, with respect to the nature of the microscopic *motion* taking place in the material, between Figs. 1.6*a* and 1.6*b*, on the one hand, and Fig. 1.6*c*, on the other hand. In Figs. 1.6*a* and 1.6*b*, the atoms are immobilized except for *vibrational* motions (Fig. 1.7*a*) about their average positions. In Fig. 1.6*c*, the atoms are free to make long, uninhibited, *translational* excursions. Macroscopically, this is nothing less than the distinction between *solidity*, on the one hand, and *fluidity* (in the extreme form exhibited by a dilute gas), on the other hand. In a solid, the atoms oscillate about equilibrium positions, which constitute a durable structure. No such enduring structure exists in a fluid, in which the atomic motion is characterized by extensive translational movements.

The fluid of Fig. 1.6*c* is a gas. In a dense fluid, that is, a liquid, translational movement is likewise an essential characteristic of the atomic motion. Since each atom is now hemmed in to a substantial extent by nearby atoms,

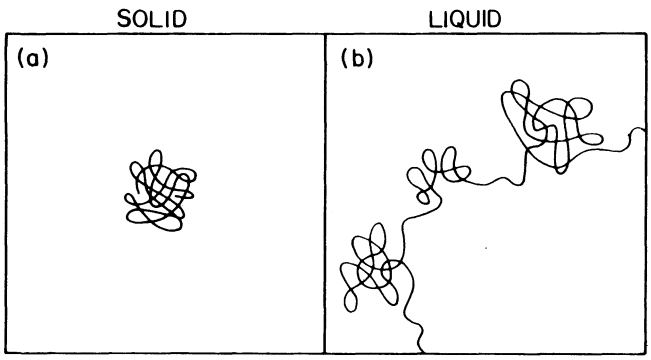

Figure 1.7 Sketches of the state of atomic motion (*a*) in a solid and (*b*) in a liquid.

the motion is also partly oscillatory. This is schematically represented in Fig. 1.7*b*, which is intended to convey a sense of the atomic movement in a liquid. (Trajectories similar to the one sketched here appear in computer simulations of the liquid state, such as those discussed in Chapter Four.) In spite of the presence of an oscillatory component, the key feature is the presence of a translational component of motion. A liquid, like a gas, possesses no enduring arrangement of atoms. Each atom in a liquid is mobile and wanders through the material, changing neighbors continually during its diffusive meandering. Atoms in a solid retain their neighbors (aside from rare events such as vacancy jumps) as all remain near fixed positions.

Moving from these atomistic descriptions to more standard macroscopic definitions: a liquid flows, lacks a definite shape (though its volume is definite), and cannot withstand a shear stress; a solid does not flow, has a definite shape, and exhibits elastic stiffness against shear. The distinction is usually quite clear. A glass (tumbler) of water consists of two transparent substances, one liquid and one solid. Water is our most familiar liquid, and the ease with which it flows is its most familar property. The rigid, brittle container in this example is an amorphous solid, an oxide glass related to fused silica (SiO_2). The structure (static for the glass, everchanging for the liquid) is of the type indicated in Fig. 1.6*b* for both materials, but the motion is as in Fig. 1.7*a* for the solid container and as in Fig. 1.7*b* for its fluid contents.

Amorphous solids are bona fide solids, having all of the requisite elastic properties (shear stiffness, etc.). There is no need to belabor this point, many of the applications of these materials (look ahead to Table 1.2) rely explicitly on properties such as rigidity and strength. Note that neither the macroscopic (rigidity, etc.) nor the atomic (Fig. 1.7*a*) description of solidity makes any reference to the presence or absence of structural long-range order, indeed, solidity is *not* synonymous with crystallinity.

It should not be necessary any longer to emphasize that solidity $\neq$ crystallinity. Unfortunately, it is, in fact, necessary to do so. The reason for this necessity arises from the following circumstance: Amorphous solids are rarely included in textbooks on solid-state physics. If one were tempted to define the subject of "solid-state physics" by the content of current textbooks with that title, one might erroneously conclude that solid-state physics is synonymous with crystal physics. So much is this the case, in fact, that it is standard procedure for a course on the physics of solids to begin with a discussion of crystal lattices and translational periodicity *as if periodicity were a prerequisite for solidity.* Since it blithely ignores an entire important class of solids, this attitude is completely wrong.

This mistaken premise, the exclusive association of solidity with crystallinity, brings us to the third in the troika of topics listed in the title of this section. This topic has to do with the issue of the *respectability* of amorphous solids as proper inhabitants of the solid state. This issue arises as a historical legacy, and it is likely to fade with time into a non-issue as it becomes impossible for new (or revised) solid-state-physics texts to ignore the scientific and

technological significance of glasses. Symptomatic of the inevitable respectabilization (and helping to hasten the process along) was the 1977 Nobel Prize in Physics shared by P. W. Anderson, N. F. Mott, and J. H. Van Vleck. Anderson and Mott were recognized, in part, for their deep contributions to the theory of amorphous solids, some of which are described in Chapter Five.

Although reluctance to accept amorphous solids as an integral part of solid-state physics is an attitude that will (hopefully) disappear before long, it is instructive to consider the factors which contributed to that misguided attitude. There is no mystery here. Solid-state physicists have traditionally been raised on the mathematical amenities of translational periodicity. Much of the machinery of familiar solid-state theory explicitly depends on and exploits the presence of long-range order in the crystalline solid state. This theoretical machinery includes: Brillouin zones, Bloch functions, **k**-space, $E(\mathbf{k})$ electronic band structures, $\omega(\mathbf{k})$ phonon dispersion curves, and elegant uses of symmetry and group theory for the labeling of eigenstates and the elucidation of selection rules. In the amorphous solid state, the loss of long-range order severely reduces, and possibly eliminates, the validity and utility of the above-mentioned mathematical tools. This must seem like Paradise Lost to many theorists, and it accounts for the past reluctance of some to face the reality of noncrystalline solids. But, however essential it may be to many standard theoretical techniques, long-range order is simply *inessential* to an entire class of solids—which do very well without it.

It is sometimes emphasized that an amorphous solid is metastable with respect to some crystalline phase that forms the thermodynamic equilibrium state of lowest energy. While this statement itself is correct (though no general proof of it exists), the emphasis is misplaced because experience teaches that the crystalline ground state is normally kinetically inaccessible. Once formed, glasses can persist without practical limit ($> 10^n$ yr). The situation is similar to that of crystalline diamond. Diamond, the hardest substance known and the archetypal covalent crystal, is metastable. The lowest-energy configuration of a collection of carbon atoms is not as diamond but as graphite, which is the stable thermodynamic phase at standard temperature and pressure. Despite their metastability, "diamonds are (effectively) forever"; a diamond is in no danger, and persists indefinitely at STP. Since the same is true of a glass well below T_g, metastability becomes an academic matter.

1.4 THE GLASS TRANSITION

Phenomena associated with the liquid↔glass transition are macroscopic manifestations of the crossover between the two microscopic motional situations of Fig. 1.7. Some aspects of the glass transition have already been shown in Figs. 1.1 and 1.2. This section presents further phenomenological aspects associated with T_g. In particular, the question of an underlying *equilibrium* thermodynamic transition is addressed.

The basic thermodynamic response function to be experimentally examined in connection with a temperature-induced change of phase is C_P, the specific heat at constant pressure. C_P measures the heat absorption from a temperature stimulus, and is defined by $C_P \equiv (dQ/dT)_P = T(\partial S/\partial T)_P$. Here dQ is the heat absorbed by a unit mass of the material to raise its temperature by dT, and S is its entropy.

Figures 1.8 and 1.9 show $C_P(T)$ data for two very different amorphous solids, the covalent glass As_2S_3 and the metallic glass $Au_{0.8}Si_{0.1}Ge_{0.1}$. In each case, the glass transition clearly appears as a "step" in the specific heat. For As_2S_3, $C_P(T)$ can be followed continuously from low temperature up through T_g and well into the liquid regime to T_f and beyond. For $Au_{0.8}Si_{0.1}Ge_{0.1}$, a portion of the liquid curve (shown dashed in the figure) is extrapolated between measured values taken just above T_g and just below T_f, because crystal-

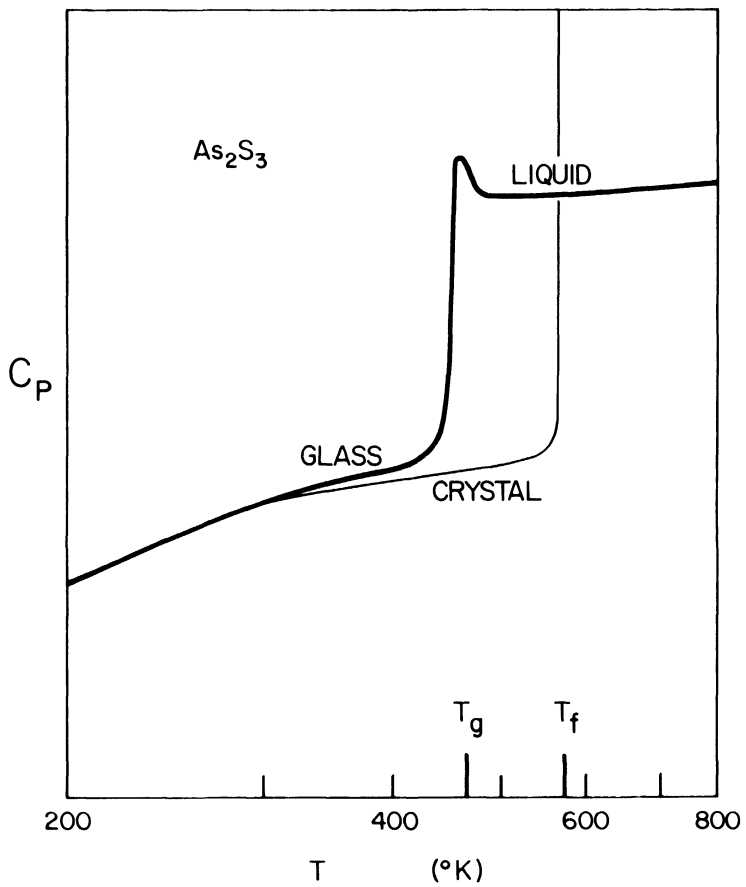

Figure 1.8 The specific heat of the crystalline, amorphous, and liquid forms of As_2S_3, a covalent material which is a prototypical glass former (after Blachnik and Hoppe, 1979).

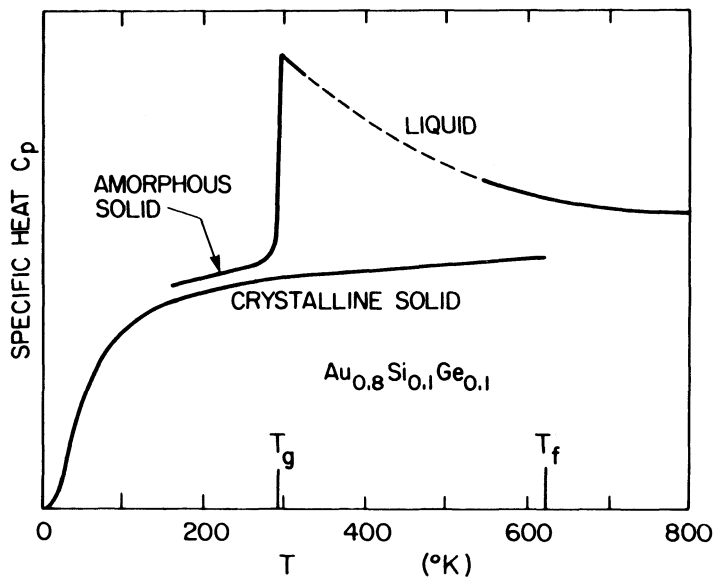

Figure 1.9 The specific-heat signature of the glass transition in a metallic glass (Chen and Turnbull, 1968).

lization intervenes shortly after passing these temperatures at the relatively slow heating or cooling rates required for measuring C_P. Figure 1.9 is of historic interest because it provided the first thermodynamic evidence of a glass transition in an amorphous metal, observed upon warming a splat-quenched sample through T_g (Chen and Turnbull, 1968).

Included in Figs. 1.8 and 1.9 are the specific heat curves for the crystalline forms. For each material, the values of C_P(glass) and C_P(crystal) are similar. The experimental curve for crystalline As_2S_3 in Fig. 1.8 is followed to the melting point T_f, where C_P diverges because of the heat of fusion—the latent heat (finite ΔQ with $\Delta T = 0$) associated with the crystal ↔ liquid transition. No such latent-heat singularity accompanies the glass ↔ liquid transition.

The behavior of $C_P(T)$ near T_g in Figs. 1.8 and 1.9 is qualitatively the same as that of $\alpha(T)$ in Fig. 1.2: Both the specific heat and the thermal expansion coefficient step up, in a narrow temperature interval, from a low value characteristic of the glass to a high value characteristic of the liquid. This behavior is very close to that expected for a second-order transition, as now discussed.

A phase transition is said to be first order if the volume and entropy (which are first-order derivatives, with respect to pressure or temperature, of the thermodynamic Gibbs function) change discontinuously. Crystallization is the prime example of a first-order transition: The volume discontinuity at T_f is illustrated in Fig. 1.1, the entropy discontinuity corresponds to the heat of fusion. A transition which is continuous in V and S is said to be second order or

higher, nth order if the nth derivatives of the Gibbs function are the lowest ones to show a discontinuity. A second-order transition thus involves discontinuities in quantities such as the slopes of $V(T)$ and $S(T)$, i.e., $\alpha(T)$ and $C_P(T)$.

From the above definition and from the behavior observed near T_g in Figs. 1.1, 1.2, 1.8, and 1.9, it may be seen that characteristic properties of the glass transition closely resemble a second-order thermodynamic transition. While $V(T)$ is continuous through the vicinity of T_g (Fig. 1.1), $\alpha(T)$ and $C_P(T)$ definitely change their values upon passing through this region (Figs. 1.2, 1.8, 1.9). However, these changes are not sharp (as they should be in a true second-order transition) but instead are *diffuse*, occurring over a small temperature interval rather than at a single sharply definable temperature. Thus the kink in $V(T)$, separating the undercooled liquid from the amorphous solid in Fig. 1.1, is rounded, so that the corresponding step in $\alpha(T)$, while steep, is not a vertical discontinuity. Similar statements apply to the bend in the entropy function $S(T)$ and to the corresponding step in the specific heat $C_P(T)$. Nevertheless, the steps exhibited near T_g in Figs. 1.8 and 1.9 are certainly quite clear and pronounced. It is therefore convenient, in order to further distinguish the solidification transition which occurs at T_g from that which occurs via crystallization (in a true first-order transition) at T_f, to phenomenologically characterize the liquid $\leftrightarrow$ glass transition as an *apparent, diffuse, second-order transition*. This characterization is a useful mnemonic that helps to flesh out the continuous/discontinuous dichotomy already noted with respect to the phase-change events at T_g and T_f. It also emphasizes the fact that, in thermodynamic measurements such as those shown in Figs. 1.2, 1.8 and 1.9, the glass transition is well defined.

The above discussion dwells on thermodynamic aspects of the glass transition. Kinetic aspects of this transition are also important. The influence of $\dot{T}$ on the observed transition, illustrated previously in Fig. 1.2, is the clearest proof that the event actually observed near T_g differs from a strict second-order transition. The shift of T_g with $\dot{T}$, understood (as discussed in Section 1.1) in terms of the interplay between the time scale of the experiment and the kinetics of molecular recovery, is the main manifestation of the kinetic dimension of the glass transition. But there are other effects, some of which can be quite subtle. For example, it is typically found that bringing a glass to a temperature just below T_g—and holding it there for differing lengths of time—produces definite changes in the $C_P(T)$ anomaly observed on subsequent heating. Thus the small peak that is superimposed on the step seen in C_P for As_2S_3 in Fig. 1.8 can be made more pronounced, in this way, by long annealing times near T_g. Also, the $V(T)$ characteristics represented in Figs. 1.1 and 1.2 follow the contraction of the material upon cooling. There is a small but real asymmetry between contraction and expansion, so that a slightly different shape (describable as an "overshoot" effect) is sometimes seen upon heating as $V(T)$ turns the corner at T_g.

The confluence of both the thermodynamic and the kinetic dimensions of the liquid↔glass transition presents one of the most formidable problems in condensed matter physics, and it cannot be said that there yet exists a completely satisfying theoretical description of the glass transition. The two best-known theoretical treatments, both of which adopt an equilibrium thermodynamic viewpoint, are the polymer-configuration model of Gibbs and DiMarzio (1958) and the free-volume model of Turnbull and Cohen (1961, 1970). A discussion of the free-volume model (which may be more general, and is certainly simpler, than the configurational-entropy theory designed specifically for polymers) is presented in Chapter Five, in a recent format that makes use of percolation theory.

Although kinetic effects are important in all practical observations of the transition between the amorphous solid and the liquid phase, both the Gibbs–DiMarzio and the Turnbull–Cohen theories previously cited reflect the following prevalent view of the glass transition: There exists an *underlying thermodynamic transition* that is intimately related to T_g. While kinetics intervenes to influence the placement of T_g in a particular set of experimental circumstances, T_g never strays very far from the value corresponding to the underlying transition.

Strong empirical support for the idea that the observed glass transition is the kinetically modified reflection of an underlying equilibrium transition (which is presumed to be close to second order in character) is contained in data of the type displayed in Fig. 1.10. The curve shown here, obtained by integrating $C_P(T)$ specific heat data (such as that shown in Figs. 1.8 and 1.9) for the hydrogen-bonded glass-forming liquid $H_2SO_4 \cdot 3H_2O$, tracks the entropy $S(T)$ of the liquid from the melting point down to T_g. The quantity plotted is the excess entropy $S_{ex} = S_{liq} - S_{xtl}$, the amount by which the entropy exceeds that of the crystal at the same temperature. As the temperature decreases from T_f to T_g, S_{ex} drops sharply, which comes from the fact that, just as in Fig. 1.8, the specific heat (and thus dS/dT) of the liquid is substantially larger than that of the crystal. Data are not shown here for the glass ($T < T_g$), but since we know that both the crystalline and amorphous solids have nearly equal specific heats (e.g., Fig. 1.8), it follows immediately that S_{ex} levels off at low temperatures to a nearly constant value close to $S_{ex}(T_g)$.

The significant point about Fig. 1.10, the key feature which bears materially on the question of an underlying thermodynamic transition, is the dashed line that extrapolates the liquid curve below T_g. This part of the curve, of course, was not measured, solidification having occurred when the temperature decreased past T_g. However, were we to adopt a view of the glass transition as a purely kinetic phenomenon, then it would be possible to probe the dashed curve by shifting T_g to lower temperature and thereby extending the life of the liquid phase. To do this, one would choose a slower cooling rate so that a lower temperature would be reached before the microscopic time scale (τ, as schematically at the top of Fig. 1.1) became commensurate with the ex-

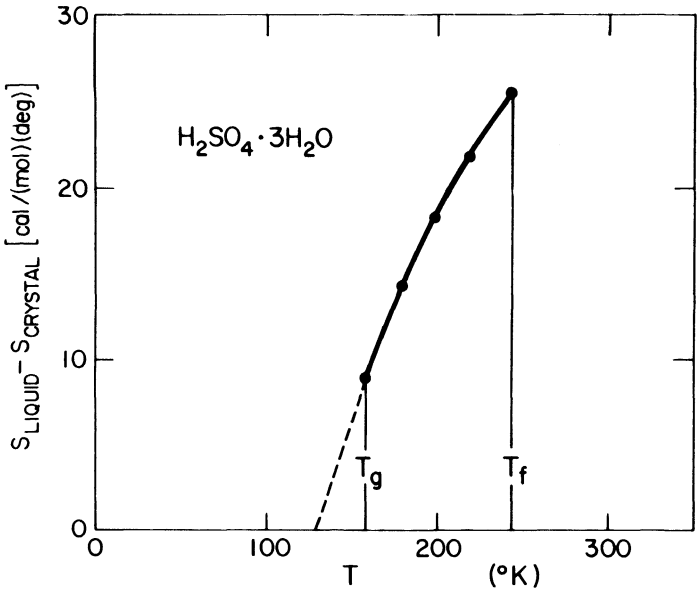

Figure 1.10 The excess entropy of a glass-forming liquid in the region between T_f and T_g, showing the extrapolation to zero excess entropy at a temperature near T_g (Angell and Sichina, 1976).

perimental time scale. Assuming infinite time at one's disposal (as well as an infinite barrier to crystallization, so that this alternative channel to the solid state is closed off), it would be possible to continue this procedure indefinitely, downshifting T_g as much as one liked and extending the liquid line down along the dashed curve of Fig. 1.10. But Fig. 1.10 shows that, even "in principle," T_g *cannot* be downshifted indefinitely. At a temperature not far from the observed T_g in Fig. 1.10, and still quite far from $T = 0$, the extrapolated entropy of the liquid becomes less than that of the crystalline solid: $S_{ex} < 0$. Since the existence, at the same temperature, of an amorphous phase (here, the liquid) with lower entropy than the stable crystalline phase is physically implausible, the extrapolated curve *cannot* be followed beyond the temperature $T(S_{ex} = 0)$ at which the excess entropy vanishes. Let us denote the vanishing-excess-entropy temperature, $T(S_{ex} = 0)$, by T_0. As the liquid is cooled, something "has to give" before this temperature is reached; the liquid phase cannot exist below T_0. What "gives" is the glass transition; the liquid solidifies to the glassy phase, and the plummeting entropy is arrested at a small positive value vis-à-vis the crystal.

Recognition of the liquid↔glass transition as an *entropy crisis* was long ago appreciated by Kauzmann (1948), and the low-temperature ($T < T_0$) extrapolation of the liquid to the physically unacceptable condition of negative excess entropy ($S_{liq} < S_{xtl}$) was later mislabeled as Kauzmann's "paradox."

Nature averts the "paradox" by interceding with solidification at T_g, thereby putting an end to the liquid state at a temperature above T_0. T_0 may be regarded as a limiting value that sets a lower bound (no matter how slow the cooling rate) on T_g. Thus do thermodynamic constraints strongly limit the influenced of kinetic effects upon T_g since $T_g \to T_0$ as $\dot{T} \to 0$. (As Gibbs and DiMarzio put it in 1958: "The existence of glasses is *not* dependent on kinetic phenomena.") Moreover, since the excess entropy of the glass must itself remain nonnegative at low temperature, the $S_{ex}(T)$ characteristic must turn *sharply* from its steep behavior above T_g (the liquid characteristic illustrated in Fig. 1.10) to its flat behavior below T_g. In other words, the glass transition cannot be *arbitrarily* gradual; it must be sharp enough to turn the corner formed by the intersection of the dashed curve with the horizontal axis in Fig. 1.10. This is why the steps [in $C_P(T)$ at T_g] in Figs. 1.8 and 1.9 are so well defined.

To summarize the argument, the presence of $T(S_{ex} = 0) \equiv T_0$ just below T_g implies the existence of a thermodynamic transition underpinning the observed liquid↔glass transition. The liquid phase simply cannot survive below T_0, and the inevitable solidification takes place at T_g which is shifted upward from T_0 by the mediation of kinetic effects. Note that the residual entropy of the glass is small, not substantially larger than that of the crystal. Although the configurational arrest that occurs at T_g freezes the liquid into one specific amorphous structure selected from a large number of similar structures, these structures are mutually inaccessible below T_g. Upon unlocking the structure of the glass by heating back into the liquid state above T_g, the equivalent disordered structures recover their mutual accessibility (via the diffusive motion of Fig. 1.7*b*), and the entropy increases accordingly.

In this discussion, entropy has been taken to be the determining thermodynamic function. Earlier, volume (or density) was used to introduce T_g in Figs. 1.1 and 1.2, because V is a much simpler quantity than S and is more easily accessible experimentally. An extrapolated temperature $T(V_{ex} = 0)$, a temperature of vanishing excess volume defined in analogy to $T(S_{ex} = 0) \equiv T_0$, is a less suitable benchmark than T_0 for the underlying transition. Nevertheless, there is a connection between V_{ex} and S_{ex}, as can be seen by the following crude argument. Model the condensed system by N atoms distributed among $N + m$ identical cells in the usual combinatorial shell game. The number of ways of placing the atoms among the cells (one or none in a cell) is $W = (N + m)!/(N!m!) = N(N - 1)(N - 2) \cdots (N - m)$. Very crudely, for $N \gg m \gg 1$, $W \sim N^{m+1}$ so that $S = k \ln W \sim k(m + 1) \ln N \sim km \ln N$. Thus S is roughly proportional to m. If we assume that thermal expansion increases the volume by increasing m (i.e., by adding more "holes"), then this proportionality relates S to the increase in V. Interpreting $m = 0$ as the high-density low-entropy locked-in state, this relation becomes $S_{ex} \propto V_{ex}$. Hence, in this drastically simplified picture (in which S amounts to the "entropy of mixing" of filled and empty cells), the excess entropy and the excess volume are closely connected. This connection (though not the simple proportionality) persists in more realistic models.

There is another facet to T_0, which concerns the viscosity η, a property of the liquid whose steep increase with decreasing temperature is often measured in the approach to the glass transition. The fact that η can be adjusted continuously from enormous (solidlike) values near T_g to moderate values at somewhat higher temperatures (a viscosity range inaccessible in the melting of a crystalline solid at T_f, in which the solid transforms abruptly to a mobile low-viscosity liquid) is of great practical importance in the technological applications of amorphous solids. (Glassblowing is the most familiar example of the usefulness of the ability to "tune" the viscosity of the melt.) Since such applications are about to be discussed in the following section, it is appropriate to make the phenomenological connection to viscosity at this point. For many materials, over much of the temperature range from T_f to T_g, the following relation has been found to describe the steep (by $>10^{12}$) rise in viscosity with falling temperature: $\eta = A \exp[B/(T - T_0)]$. This empirical equation for the temperature dependence of the viscosity is known as the Vogel–Fulcher equation, and it contains a characteristic temperature T_0 (at which η diverges) that is found to correlate well with the T_0 that has been discussed in this section.

1.5 APPLICATIONS OF AMORPHOUS SOLIDS

Ever since (and even before) the Phoenicians built a large export-oriented glassworks industry on the quartz-rich sands of the Lebanese coast, technological uses of amorphous solids have been a factor in human affairs. Books can be (and have been, e.g., Rawson, 1980) written on the applications of glasses. The quick survey given in this section is intended to convey a sense of the scope and variety of these technological uses.

Table 1.2 presents a representative list of present-day applications (or potential applications, at this writing, in the case of the last two entries) of amorphous solids. The application itself is given in the third column of the table. The first two columns show the type of glass used in the application and a specific example of such a material, while the last column indicates properties of the solid that are exploited in the application.

Traditionally, the most familiar format is as a structural material, ordinary "window glass." This architectural usage of a variety of glasses that are based on fused silica (SiO_2) exemplifies two general aspects common to many applications of amorphous solids. In the first place, as alluded to at the end of the last section, these materials *harden continuously* with decreasing temperature near T_g. The ability to control the viscosity (and thereby the flow properties) of the melt provides a valuable processing advantage in the preparation of products formed from glasses. In this way *the phenomenon of the glass transition is itself technologically significant.* Secondly, when an amorphous solid can be used in place of a crystalline one in an application calling for large-area sheets or films, it is generally advantageous to do this and thereby avoid the problems associated with polycrystallinity or the expense of preparing large single crys-

TABLE 1.2 Some examples of applications of amorphous solids

Type of Amorphous Solid	*Representative Material*	*Application*	*Special Properties Used*
Oxide glass	$(SiO_2)_{0.8}(Na_2O)_{0.2}$	Window glass, etc.	Transparency, solidity, formability as large sheets
Oxide glass	$(SiO_2)_{0.9}(GeO_2)_{0.1}$	Fiber optic waveguides for communications networks	Ultratransparency, purity, formability as uniform fibers
Organic polymer	Polystyrene	Structural materials, "plastics"	Strength, light weight, ease of processing
Chalcogenide glass	Se, As_2Se_3	Xerography	Photoconductivity, formability as large-area films
Amorphous semiconductor	$Te_{0.8}Ge_{0.2}$	Computer-memory elements	Electric-field-induced amorphous ↔ crystalline transformation
Amorphous semiconductor	$Si_{0.9}H_{0.1}$	Solar cells	Photovoltaic optical properties, large-area thin films
Metallic glass	$Fe_{0.8}B_{0.2}$	Transformer cores	Ferromagnetism, low loss, formability as long ribbons

tals. Thus it would be prohibitively expensive to fabricate large windows out of crystalline SiO_2 (quartz), while it is eminently feasible to do so using SiO_2-based silicate glasses.

Of course, besides the above general advantages, which have to do with practicality of preparation, it is also true that silicate glass is far superior to crystalline quartz in this application, which is the first entry in Table 1.2. Although both materials are transparent to visible light, the glass is optically isotropic while quartz is optically anisotropic—a drawback in a window material. Moreover, the glass is a far better thermal insulator, and a window should keep heat and cold out as well as let light in. Both the optical isotropy and the low thermal conductivity are the consequences of disorder in a nonmetallic amorphous solid. Isotropy results because no special (i.e., symmetry) directions survive the loss of long-range order, while low thermal conductivity results because of the disorder-induced scattering of thermal phonons.

The Phoenicians are credited with being the first to fabricate transparent glass, and the second application entered in Table 1.2 represents a modern development of their achievement which carries it to a phenomenal level. The transparency of the glasses developed for fiber-optic communications is so great that, at certain wavelengths, light can pass along a path within the material that is a kilometer long and yet retain over 90% of its intensity.

Copper wires transmitting electrical signals presently carry most of the telephone messages transmitted around our planet, but it seems likely that this function will someday be carried out largely by glass fibers transmitting optical signals. Bell himself, in 1880, demonstrated a "photophone" in which he used the voice-induced motion of a reflecting diaphragm to modulate a light beam and transmit a signal through the air to a photoreceptor 200 meters away. At that time, the absence of a convenient low-loss conduit for the light (the atmosphere is unreliable as an optical-transmission medium) prevented light-wave communications from progressing further. What has made this idea practical now is the availability of glass fibers of such purity and homogeneity that their optical attenuation is so low (<0.3 decibels/kilometer) as to make them ideal conduits for the light.

Essential aspects of the use of glass fibers in telecommunications networks are schematically shown in Fig. 1.11. Electrical pulses produced by pulse-code modulation from speech in a telephone system (or digitally encoded pulses originating from a computer in other kinds of information-transmitting systems) are converted into a similar sequence of light pulses by a semiconductor laser or light-emitting diode coupled to one end of the optical fiber. The signal is transmitted along the fiber as a stream of light pulses, and at the other end it is converted back into electrical pulses and then finally into the desired form (speech, printed output, computer file, etc.).

The hairlike glass fiber, about 100 μm in diameter, functions as a light-guide—a waveguide in the optical portion of the electromagnetic spectrum. The simplest type is illustrated at the upper left of Fig. 1.11. A central core of ultratransparent glass is sheathed by a coaxial cladding of a glass having a

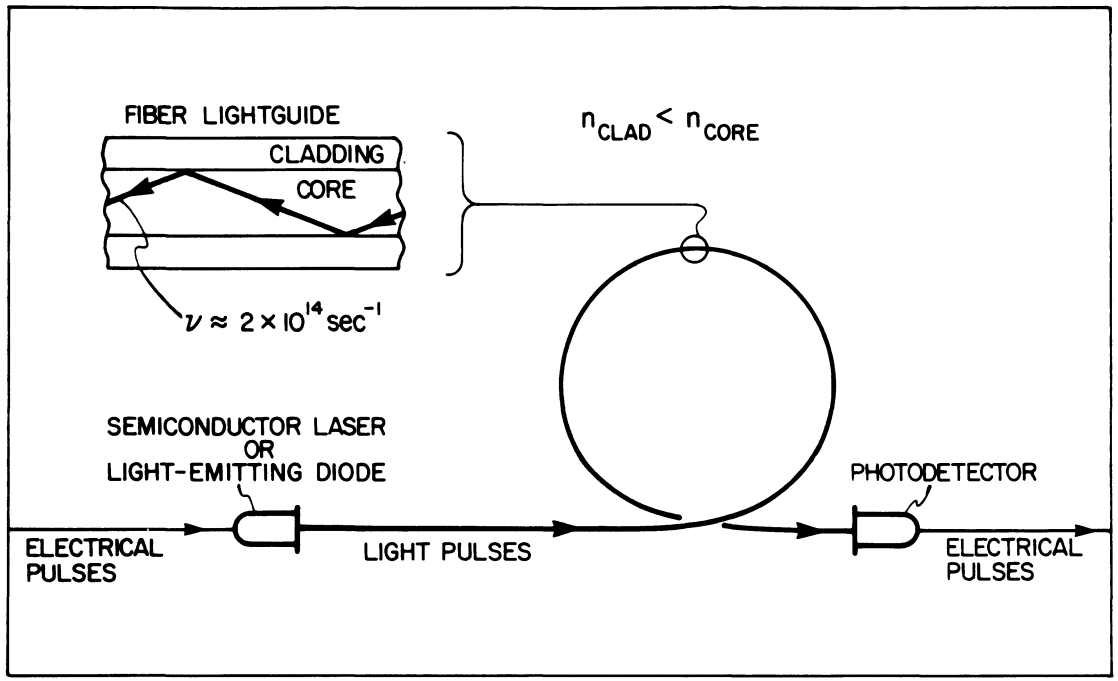

Figure 1.11 The use of ultratransparent glass fibers in telecommunications networks.

refractive index lower than that of the core. Because $n_{\text{cladding}} < n_{\text{core}}$, light rays propagating within the core at small angles relative to the axis are totally internally reflected at the core/cladding interface and remain confined within the lightguide core. Typical materials used for the core are silica–germania glasses such as the one listed in Table 1.2, and the cladding can be a similar glass of somewhat different composition. Careful control of composition makes it possible to construct "graded-index" fibers in which the refractive index falls off radially from the core axis in a predetermined profile designed to keep the light pulses from spreading out as they travel down the guide. In the simple stepped-index configuration shown in Fig. 1.11, different optical modes would propagate with different velocities along the fiber (sharply angled zigzag paths are longer, and travel slower, than zigzag paths more parallel to the axis). Graded-index fibers are tailored to elegantly cancel out this "mode dispersion," so that the light pulses are transmitted down the guide without distortion.

The substitution in communications networks of optically transmitting glass wires for electrically conducting crystalline wires is driven by several advantages of the fiber lightguides. Light losses are so low that "repeater" spacings can be much larger than for metal-conductor systems. ("Repeaters" are receiver/transmitter elements that periodically rejuvenate the pulses along long lines.) More fibers (even clothed in their protective polymer packaging) than copper wires fit into a cable of given size. Optical fibers also have negligible crosstalk and are immune to electromagnetic interference. But by far the most significant advantage of an optical communications system is its information-transmitting capacity, which is far higher than that of a conducting system. This high capacity derives from the very high frequency (about 2×10^{14} sec^{-1} for operation at a wavelength of 1.5 μm, a typical wavelength in the near-infrared ultratransparent "window" of the glass) of the lightwave carrier, which allows it to be modulated at very high frequencies. Much more traffic (e.g., many more simultaneous conversations) can be borne by a glass fiber than by its copper counterpart.

The applications discussed thus far involve oxide glasses in a classic tradition. But the most ubiquitous amorphous solids in present-day society are organic glasses, polymeric solids composed of intermeshed long-chain organic molecules. These materials are represented by the third row in Table 1.2. Many of the innumerable "plastic" products in everyday use belong to this class of amorphous solid, which is now the most technologically pervasive type of glass. (On a volume basis, more plastic is now produced than steel.) Among the reasons for this enormous prominence of organic polymers as structural materials are ease of processing on a large scale (again capitalizing on thermal behavior near T_g), low cost, light weight, and high mechanical strength.

In the communications link sketched in Fig. 1.11, the role played by the glass element is one of transmission. The photoelectronic elements that bracket the optical fiber, the semiconductor-laser transmitter at one end and the photodetector receiver at the other, are both based on crystalline semicon-

ductors. In the next group of three applications listed in Table 1.2, semiconducting amorphous solids play an electronically active role.

Figure 1.12 displays the process of xerography, the most widely used form of electrophotography or electrostatic imaging. This process is the basis of most plain-paper copying machines used in offices, libraries, schools, etc., and at the heart of the process is a large-area thin-film photoconducting element (shown shaded in Fig. 1.12), which is an amorphous solid. Typical materials employed as the photoconductor are chalcogenide glasses such as Se or As_2Se_3, formed by vapor condensation on a metal substrate. These glasses are semiconductors with bandgaps of about 2 eV, transparent in the infrared but highly absorbing for visible light (photon energy $h\nu$ in the range from 2 to 3 eV).

The steps in the xerographic (literally "dry writing") process are schematically represented in the four-part sequence of Fig. 1.12. In the dark, the photoconductor is a good insulator, and while in this state its surface is uniformly charged by ions from a corona discharge, as indicated in Fig. 1.12*a*. An equal and opposite induced charge develops at the metal-photoconductor interface. The chalcogenide film, about 50 μm thick, supports an electric field in excess of 10^5 V/cm.

The imaging step is shown in Fig. 1.12*b*. The photoconductor plate is exposed to a pattern of visible light in the form of an image reflected from the document being copied. Where light strikes the photoconductor, photons are absorbed and electron-hole pairs are created by excitation across the energy gap. Photogeneration of mobile charge carriers is assisted by the large electric field present, which helps to pull apart the mutually attracting electron and hole of each light-created pair so that each charge is free to move separately. The electrons then move under the influence of the field to the surface, where they neutralize positive charges located there, while the holes move to the photoconductor–substrate interface and neutralize negative charges located there. Where intense light strikes the photoconductor, the earlier charging step of Fig. 1.12*a* is totally undone; where weak light strikes it, the charge is partially reduced; and where no light strikes, the original electrostatic charge remains on the surface. The optical image has been converted into a latent image consisting of an electrostatic potential distribution that replicates the light and dark pattern of the original document.

To develop the electrostatic image, fine negatively charged pigmented particles are brought into contact with the plate. These "toner" particles are attracted to positively charged surface regions, as shown in Fig. 1.12*c*. The toner is then transferred, in a step illustrated in Fig. 1.12*d*, to a positively charged sheet of paper. Brief heating of the paper fuses the toner (an organic glass) to it and produces a permanent photocopy. To prepare the photoreceptor for the next copy, remaining toner is cleaned off and the residual electrostatic image is erased (i.e., discharged) by flooding with light. In high-speed duplicators the photoconductor layer is usually in the form of a moving continuous drum or belt, around the perimeter of which are located stations for performing the functions of Fig. 1.12. The advantage of an amorphous semi-

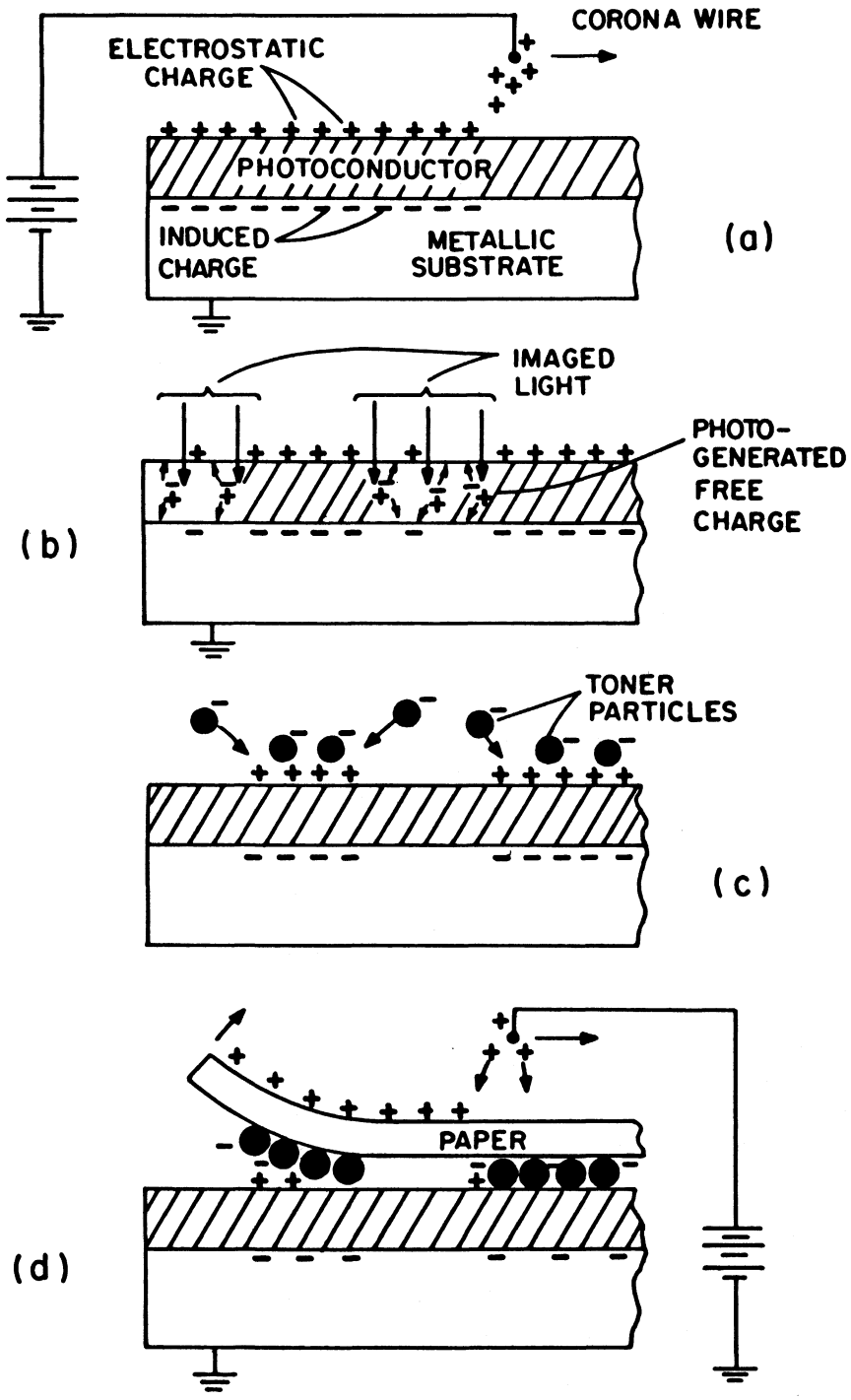

Figure 1.12 The use of amorphous semiconductors as large-area photoconducting layers in xerography. Steps in the xerographic process include (*a*) charging, (*b*) exposure, (*c*) development, and (*d*) transfer.

conductor for the photoconductor layer in this application resides largely in the ability to prepare uniform large-area thin films of amorphous materials. The speed of xerographic printing technology is presently on the order of several copies per second.

The application of tellurium-rich semiconducting glasses as computer-memory elements, the fifth entry in Table 1.2, exploits a phenomenon specific to amorphous materials. This is electric-field-induced crystallization of the glass. For Te-rich Ge-Te glasses, the crystal→glass transformation results in a large ($\times 10^6$) increase in electrical conductivity because, although both the crystalline and amorphous forms are semiconductors, the bandgap of the crystalline form is very small in this system. A current pulse converts the low-conductivity glass to the high-conductivity crystal; in computer terms, the pulse "switches" the material from the "off" to the "on" state (Adler, 1977; Ovshinsky, 1968). What is interesting is that the "off" state may be restored by another short pulse of current; the glass↔crystal transition is electrically reversible for these materials.

Although not yet completely understood, the reversible switching phenomenon may be visualized in the following way. The off→on glass→crystal transition results from heating the glass to just above T_g, where crystallization occurs readily for this system, and produces filamentary conducting paths of crystalline material which span the film thickness. The current pulse which triggers the on→off crystal→glass reverse transition does this by melting the crystalline filaments (taking them above T_f). The molten filaments are then quenched (taken below T_g) so quickly by the surrounding material that the glass is re-formed, returning the film to the low-conductivity off state. (This description suggests the possibility of using short laser pulses in place of current pulses, and such optically driven switching is indeed an interesting variation of this phenomenon.) Devices based on these films are used as electronically alterable ("read-mostly") memories in computer applications.

The ultimate application of large-area photoreceptor films is clearly in the field of solar energy. If solar-cell technology is ever to contribute an appreciable fraction to worldwide energy production, many hundreds of square miles of the planet's land area will need to be turned over to such "sun-harvesting" activity (Mort, 1980). Amorphous materials, such as polymers, immediately suggest themselves for an application calling for large-area films in such quantity. The example given in Table 1.2 is amorphous silicon, an interesting long-term candidate for solar-cell technology.

Crystalline silicon, of course, is of overwhelming importance in the electronics industry. While crystalline silicon photovoltaic cells are used to power equipment on space-probe vehicles, this material is too expensive for use on the scale envisaged here. Amorphous silicon, on the other hand, can be prepared in large-area films at a far lower cost than its crystalline counterpart. Moreover, a very thin film (~ 1 μm) of *a*-Si suffices to absorb most of the solar-spectrum light, while a much thicker film (>50 μm) of *c*-Si is required for this purpose. (*Note*: When the amorphous and crystalline forms of a given

solid are discussed side by side, the prefixes *a-* and *c-* will often be used to distinguish them.) The reason for the much higher optical absorption of *a*-Si is the disorder-induced breakdown of the optical selection rules that control interband transitions in the crystal. (This consequence of disorder is described in Chapter Six.)

As noted in Table 1.2, the material of interest with respect to solar-cell technology is not pure amorphous silicon but is instead an amorphous alloy containing appreciable hydrogen (usually written *a*-Si:H). The superiority, as an electronic material, of hydrogenated amorphous silicon over the pure material, is an interesting scientific story—to be discussed in Chapter Six. In brief, the role of hydrogen is to eliminate electronic defects ("states in the gap") which are intrinsic to elemental *a*-Si.

The final entry in Table 1.2 is one of the applications of metallic glasses formed by the melt-spinning technique of Fig. 1.3. One of the attractions of these metal glass ribbons is that they are cast directly from the melt in a swift, single-step process. Conventional methods needed to manufacture crystalline metal in thin-strip form call for a complex sequence of steps involving casting, hot-rolling, cold-rolling, and annealing, and consume about five times as much energy as melt spinning of glassy ribbon. One of the earliest (circa 1978) commercial uses of these ribbons was in the form of a nickel-based brazing alloy employed in building aircraft engines. However, the main potential of these glasses, as indicated in the last line of Table 1.2, is in their use as magnetic materials.

Ferromagnetic glasses such as $Fe_{0.8}B_{0.2}$, $Fe_{0.7}P_{0.2}C_{0.1}$, and $Co_{0.8}Fe_{0.1}B_{0.1}$ combine high saturation magnetization with the useful property of being "magnetically soft" (low coercivity, easily magnetized by small magnetic fields). Crystalline ferromagnets that are magnetically soft are also, unfortunately, mechanically soft, but the glass ferromagnets mentioned here are found to be quite hard. Also, the magnetic glasses are isotropic, and the absence of a crystalline axis of easy magnetization allows the magnetization direction to be rotated at a much smaller energy cost than in crystals. The high (relative to crystalline metals) electrical resistivity of amorphous metals is also helpful in this regard. For these reasons, ferromagnetic glasses are under active development for use in the magnetic cores of power transformers, where their low-loss properties are very important. Other potential applications of amorphous metal magnets are in magnetic disk memories and read/write recorder heads.

It is a mainstream tradition in solid-state physics that much scientific insight follows in the wake of research motivated by the technological importance of a class of materials (as with crystalline semiconductors after the invention of the transistor), and amorphous solids—which had practical utility long before they acquired scientific respectability—fit well into that tradition. The applications listed in Table 1.2, as well as others omitted for lack of room, have contributed greatly to progress in the physics of amorphous solids.

This survey of applications of glasses has contained within it a brief over-

view of physical properties: mechanical, optical, electronic, and magnetic. It is noteworthy that the paragraph before last casually began with the term "ferromagnetic glasses." The occurrence of *ferromagnetism* among amorphous solids comes as a shock to any physicist who insists upon identifying this distinctive solid-state property as an exclusive consequence of crystalline order. There are also *superconducting* glasses; examples are bismuth, gallium, $Pb_{0.9}Cu_{0.1}$, and $La_{0.8}Au_{0.2}$. Superconductivity and ferromagnetism in the amorphous solid state exemplify a main theme of this book. Mentioned earlier (Section 1.3) but worth repeating, this is the *inessentialness of long-range order in solids.* Having done away with long-range order and translational periodicity, we now go on to analyze the disorder (*and* the remaining order) that characterizes the structure of amorphous solids.

REFERENCES

Adler, D., 1977, *Scientific American* **236**, No. 5, 36.
Angell, C. A., and W. Sichina, 1976, *Ann. N.Y. Acad. Sci.* **279**, 53.
Blachnik, R., and A. Hoppe, 1979, *J. Non-Crystalline Solids* **34**, 191.
Chaudhari, P., W. C. Giessen, and D. Turnbull, 1980, *Scientific American* **242**, No. 4, 98.
Chen, H. S., and D. Turnbull, 1968, *J. Chem. Phys.* **48**, 2560.
Gibbs, J. H., and E. A. DiMarzio, 1958, *J. Chem. Phys.* **28**, 373.
Kauzmann, W., 1948, *Chem. Rev.* **43**, 219.
Kovacs, A. J., J. M. Hutchinson, and J. J. Aklonis, 1977, in *The Structure of Non-Crystalline Materials,* edited by P. H. Gaskell, Taylor and Francis, London, p. 153.
Mort, J., 1980, *Phys. Technol.* **11**, 134.
Ovshinsky, S. R., 1968, *Phys. Rev. Letters* **21**, 1450.
Predel, B., and H. Bankstahl, 1975, *J. Less-Common Metals* **43**, 191.
Rawson, H., 1980, *Properties and Applications of Glass,* Elsevier, Amsterdam.
Turnbull, D., 1969, *Contemp. Phys.* **10**, 473.
Turnbull, D., and M. H. Cohen, 1961, *J. Chem. Phys.* **34**, 120.
Turnbull, D., and M. H. Cohen, 1970, *J. Chem. Phys.* **52**, 3038.